

## Measurement of collision-induced radiative deexcitation cross sections for metastable $\text{He}^*(2^1S)$ interacting with He, Ar, Kr, and Xe

C. Dehnbostel, R. Feltgen, and G. Hoffmann

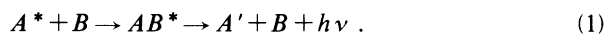
*Max-Planck-Institut für Strömungsforschung, D-3400 Göttingen, West Germany*

(Received 29 May 1990)

The radiative deexcitation cross section for  $\text{He}^*(2^1S)$  in collisions with He has been measured in the collision energy range from 40 to 110 meV. The experimental results agree well with quantal distorted-wave calculations of Zygelman and Dalgarno [Phys. Rev. A **38**, 1877 (1988)]. The measured radiative quenching cross sections for the systems  $\text{He}^*(2^1S)+\text{Ar,Kr,Xe}$  manifest a scaling law for fixed collision energy with  $\alpha^2$  as the scaling parameter, where  $\alpha$  is the static dipole polarizability of the heavier rare gas.

### I. INTRODUCTION

The strictly forbidden electric-dipole transition from an electronically excited state to each of the lower states is the cause of the long radiative lifetime of a large class of optically metastable atoms  $A^*$ . These metastable atoms play an important role in collision processes since they act as energy carriers enabling efficient reactions even at very low collision energies. During the transition state of the collision, however, these metastable atoms may lose their intrinsic radiative metastability, because the perturbing collision partner  $B$  breaks the atomic symmetry ( $O_h$ ) of  $A^*$  and reduces it to that of the molecule  $AB^*$ . Under this reduced symmetry an electric-dipole transition to a lower state  $A'$  may be fully allowed leading to molecular emission  $h\nu$  from the collisional transition state



This process is called the collision-induced radiative deexcitation (CRD) of  $A^*$  with  $B$  acting as a catalyst. The emission spectrum of CRD is either broader ("pressure broadening") or narrower than that from the spontaneous decay  $A^* \rightarrow A'$  depending on the decay mode being either a single-photon process [magnetic- or (higher) electric-multipole emission line] or a two-photon process (continuous electric-dipole emission).

The radiative lifetimes of states with electric-dipole decay are orders of magnitude longer than the time of a thermal collision. The chance of radiative decay of  $AB^*$  occurring during a single collision is thus very small ( $10^{-5}$  or less), and the values of the CRD cross section generally range below several  $10^{-3} \text{ \AA}^2$ . Only in orbiting collisions or when more complex (polyatomic) collision partners are involved, the CRD cross section can exceed these values due to the prolonged duration of the collision.

For many thermal collision systems  $A^* + B$  [e.g.,  $\text{He}^*(2^1,3S) + \text{He}$  or  $\text{O}^*, \text{S}^*, \text{Se}^*(^1S) + \text{rare gases}$ ], CRD is the only loss process for  $A^*$  in binary collisions. At sufficiently high densities of  $B$  this decay process can be very efficient although the cross sections are small. Also

in collision systems where the cross sections for other reactions of  $A^*$  with  $B$  (Penning ionization, excitation transfer, etc.) are considerably larger than the CRD cross section, CRD nevertheless may play an important role; for instance, in electrical discharges of gas mixtures  $A + B$  with a small partial pressure of  $B$ , the loss of  $A^*$  from CRD through collisions with  $A$  can fully compete with the other reactions of  $A^*$  with  $B$ .

So far, only some rate constants have been measured for CRD. The first measurement has been performed by Phelps<sup>1</sup> for the system  $\text{He}^*(2^1S) + \text{He}(1^1S)$  [ $A' = \text{He}(1^1S)$ ] using an absorption technique in the stationary afterglow. Phelps obtained a CRD rate constant of  $6 \times 10^{-15} \text{ cm}^3/\text{s}$  at 300 K which corresponds to an average cross section  $\bar{\sigma} = 3 \times 10^{-4} \text{ \AA}^2$ . Later emission studies<sup>2</sup> yielded CRD rate constants  $r(300 \text{ K}) = 4.6 \times 10^{-15}$  and  $6.8 \times 10^{-15} \text{ cm}^3/\text{s}$  giving  $\bar{\sigma} = 2.6 \times 10^{-4}$  and  $3.8 \times 10^{-4} \text{ \AA}^2$ , respectively. CRD values for  $\text{He}^*(2^1S) + \text{Ne, Ar, Kr, Xe}(^1S)$  have not been determined to date; the dominant reactions of these systems are excitation transfer and Penning ionization. The CRD rate for  $\text{He}^*(2^3S) + \text{He}(1^1S)$  is extremely small as can be expected from the metastability of the  $a^3\Sigma_u^+$   $\text{He}_2^+$  bound states; the upper limit of the CRD cross section was estimated to be  $\sim 10^{-10} \text{ \AA}^2$ .<sup>3</sup> For the heavier rare gases CRD always competes with level mixing (LM) through collision-induced fine-structure and multiplet transitions; some CRD-to-LM branching ratios have been determined.<sup>4</sup> New interest in CRD arose from its direct involvement in high energy storage laser amplifier devices using the auroral and transauroral transitions of the chalcogens.<sup>5</sup> The related average CRD cross sections for  $A^* = \text{O}^*, \text{S}^*(^1S)$ ,  $A' = \text{O}^*, \text{S}^*(^1D_2)$ , and  $B = \text{rare gases}(^1S)$ ,  $\text{H}_2, \text{N}_2(^1\Sigma_g^+)$  have been measured at 300 K and range from  $7 \times 10^{-9}$  to  $3 \times 10^{-4} \text{ \AA}^2$ .<sup>6</sup>

There are some theoretical CRD calculations for metastable rare gases,<sup>7</sup> chalcogens,<sup>8</sup> and Zn, Cd, and Hg atoms<sup>9</sup> interacting with ground-state rare gases.

We report here the first measurements of CRD cross sections in an atomic beam experiment. The collision systems studied are  $\text{He}^*(2^1S) + \text{He, Ar, Kr, Xe}(^1S)$ . The cross sections are derived from the detection of the

collision-induced emission in the extreme-ultraviolet (EUV) region. Absolute cross-section values are obtained by a simultaneous measurement of the spontaneous two-photon emission of  $\text{He}^*(2^1S)$ .

## II. APPARATUS

The cross sections to be measured are very small. Therefore a powerful  $\text{He}^*(2^1S)$  primary beam is needed. Figure 1 shows a schematic view of the apparatus. High-purity (>99.9996%) helium gas (He 5.6, Messer Griesheim), containing less than 5 parts in  $10^7$  of neon, expands through a 30- $\mu\text{m}$ -diam nozzle from stagnation pressures between 40 and 65 bars, at nozzle temperatures  $T_0$  between 120 and 930 K, into the first chamber which is pumped by a 10 000 liter/s oil diffusion pump (HS16, Varian, 12 500 liter/s for helium) backed by a 500  $\text{m}^3/\text{h}$  roots pump (RUVAC WS 501, Leybold) and a 100  $\text{m}^3/\text{h}$  fore pump (2100, Alcatel). A conical nickel skimmer, formed by galvanoplastics, (0.35-mm-diam opening, edge sharpness 0.5  $\mu\text{m}$ , overall length 25 mm, outer and inner full opening angles 22° and 18°) is situated 12 mm downstream from the nozzle sampling the central part of the supersonic beam. The kinetic energy of the He beam ( $5kT_0/2$ ,  $k$  is the Boltzmann constant) varies from 26 to 200 meV giving beam velocities  $v_1$  from 1120 to 3110 m/s; the velocity resolution  $\Delta v_1/v_1$  ranges around 2% according to Mach numbers around 100. The He atoms of the beam are excited in the second chamber by parallel electron bombardment from an electron gun which is essentially the same as that of Brutschy and Haberland<sup>10</sup> where the electron beam is optimized by positive ion trapping<sup>11</sup> and magnetic confinement.<sup>12</sup> The cathode used here is an indirectly heated tungsten dispenser cathode with a spherically shaped electron-emitting surface and a central hole (3-mm-diam) for the beam. The cathode material is a porous tungsten matrix of 80% density impregnated by a 3:1:1 mixture of Ba:Ca:Al oxide and coated by an Os-Ru addition (31 180 "M", Spectra-Mat, Inc.). Standard operating conditions of the gun are as follows:

heating voltage 7.5 V, heating current 9 A, emission 220 mA, and electron energy 300 V. This results in a 1–4% gain in beam velocity for  $\text{He}^*$  depending on  $v_1$ . Typical  $\text{He}^*$  fluxes at  $v_1=1800$  m/s are several  $10^{14} \text{ s}^{-1} \text{ sr}^{-1}$ . After the excitation region the beam passes a 300 V/cm condenser, which removes charged particles by deflection and Rydberg states by field effect. The condenser also protects the following quench lamp from the contamination. This lamp consists of a spirally shaped helium gas discharge tube wound around the beam on a length of 70 mm; the discharge current is about 20 mA at 3 kV and 3 Torr helium pressure. The 2- $\mu\text{m}$  line of the discharge enables the separation of the metastable  $2^1S$  and  $2^3S$  states by quenching the singlet component. Our metastable beam contains 92% singlet and only 8% triplet metastables. All measurements for the  $\text{He}^*(2^1S)$  state are performed by subtraction of the signals with lamp off and on. Leaving the quench lamp, the beam consists of state selected metastables, ground-state atoms and photons. In order to separate the thermal particles with a well-defined velocity  $v_1$  from the beam photons, a very simple time-of-flight (TOF) chopper of high transparency is sufficient. To avoid overlapping the chopper disk has ten slits with an opening angle of 14.4° and ten teeth with a closing angle of 21.6°, and for a given  $v_1$  the chopper frequency  $f$  is put to

$$f = 0.05v_1/s, \quad (2)$$

with  $s$  being the distance from the chopper to the collision cell where the signals caused by the beam photons and the metastables are registered during the open and closed periods of the chopper, respectively. The transparency of the chopper is 40%.

After passing a final 1000 V/cm condenser at the entrance to the third chamber, the beam enters the collision cell where the target gas can be admitted. The cell is of small compact size with 3-mm-diam entrance and exit holes, the length  $L$  of the collision region is 13 mm. A 150-nm-thick Al-1 at. % Si alloy foil (TF-101-a, Luxel Corporation<sup>13</sup>) is mounted to one side of the cell acting as a filter for EUV photons. Metal foils start to transmit electromagnetic waves for frequencies greater than the plasma frequency  $\nu_p$  which is approximately<sup>14</sup>

$$\nu_p \sim 9 \times 10^3 n^{1/2}; \quad (3)$$

$n$  is the number of electrons per  $\text{cm}^3$  that take part in the collective oscillations. Transmission in Al begins at  $h\nu=14.6$  eV (Ref. 15) corresponding to a wavelength of 85 nm. On the short side, the transmittance increases until the  $L_{2,3}$  x-ray edge at 17 nm is reached.<sup>16</sup> At 60 nm, the Al filters of Luxel have a nominal transmittance of 0.14. Behind the Al filter a channeltron (Mullard model B419BL-01, Valvo<sup>17</sup>) is mounted which counts the EUV photons  $P$ . The channeltron is hermetically surrounded by a box which is pumped through a long tube from the vacuum in the third chamber; the dark count rate of the channeltron is about  $0.01 \text{ s}^{-1}$ . Collision cell and channeltron box are integrated in one copper block and attached to a cryostat which can be cooled down to 1.5 K. In the present experiments, however, the block is kept at 300 K,

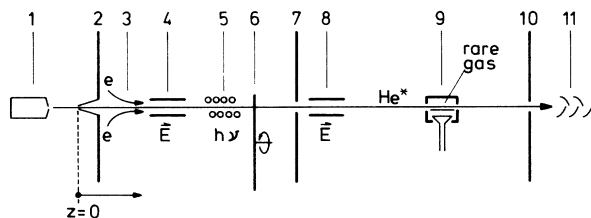


FIG. 1. Schematic view of the apparatus. 1, nozzle source (nozzle 30  $\mu\text{m}$   $\phi$ ,  $z \sim -12$  mm); 2, skimmer 0.35 mm  $\phi$ ,  $z=0$  mm; 3, electron gun; 4, condenser; 5, He quench lamp; 6, TOF chopper  $z=680$  mm; 7, collimator 4 mm  $\phi$ ,  $z=794$  mm; 8, condenser; 9, collision cell ( $z=1288$  mm) with Al filter and photon channeltron; 10, collimator 0.4 mm  $\phi$ ,  $z=1954$  mm; 11, metastable multiplier.

since the extremely small count rates for process (1) (down to less than  $1 \text{ s}^{-1}$ ) cannot be measured with a channeltron at such low temperatures due to the rapid increase of the electrical resistance of the channeltron wall.

The beam leaves the third chamber through a small hole of 0.4-mm-diam in order to reduce the high metastable intensity which is permanently monitored in the fourth chamber by a Cu-Be electron multiplier (type 9642/3A, EMI) giving the scattering rate  $S$

$$S = (I_0 - I) / I_0, \quad (4)$$

with  $I_0$  and  $I$  being the metastable intensity (particles per second) for the cell without and with target gas, respectively.

The signals from the photons  $P$  and the metastables  $I$  are counted. The pulses from the photon channeltron and the metastable multiplier are fed without preamplification directly to timing amplifiers (model 7041, Schlumberger and model 574, Ortec) which are followed by 100-MHz discriminators (model 436, Ortec). The nuclear instrument module (NIM) pulses at the output of the discriminators are differently handled for photons and metastables. Since the contribution from the beam photons to  $I_0$  and  $I$  are negligible, the NIM pulses in this case are directly counted by a preset counter (model 1008, Borer). In the collision cell, however, the beam photons give significant contributions to the photon signal; especially, when He is admitted as target gas, strong He fluorescence occurs. Therefore the NIM pulses from the collision-cell photons are sent to a computer-aided measurement and control (CAMAC) TOF module<sup>18</sup> consisting of a home-built TOF unit and a 1-MHz histogramming memory module (model 3588, LeCroy). The signal of interest, of course, is that during the closed period of the TOF chopper when the metastable atoms pass the collision cell.

### III. DETERMINATION OF ABSOLUTE CRD CROSS SECTIONS

Due to the smallness of the cross sections high scattering rates of 0.5–0.6 are necessary. Under these conditions, more than 30% of all collisions of the metastable atoms in the scattering cell are multiple elastic collisions.<sup>19</sup> For the considered collision systems, the metastables can no longer cause inelastic events after their first inelastic collision (CRD or Penning ionization), since they are deexcited to their ground state, i.e., the single collision condition is fulfilled for the inelastic collisions. Therefore the general formula for the CRD cross section  $\sigma$  reads<sup>19</sup>

$$\sigma = Q \frac{P\rho}{I_0[1 - (1-S)^\rho]}, \quad 0 < S < 1. \quad (5)$$

$P$  are the collision-induced photons per second in the cell,  $Q$  is the total collision cross section, and

$$\rho = q / Q \quad (6)$$

is the inelasticity with  $q$  being the sum of all inelastic cross sections of the collision system. Since  $\rho \ll 1$  for the systems under study, formula (5) simplifies to<sup>19</sup>

$$\sigma = Q \frac{P}{I_0 |\ln(1-S)|}. \quad (7)$$

The values of  $Q$  are taken from the literature.<sup>20</sup> In order to determine absolute values for  $\sigma$  the detection efficiencies for  $P$  and  $I_0$  must be measured, which is rather difficult. There is, however, an easier way.

Without target gas in the cell, one observes a photon signal which is quenched by the He lamp. It results from the natural two-photon decay of  $\text{He}^*(2^1S)$ .<sup>21</sup> During the passage through the cell, the number of decays per second is

$$N_\tau = I_0 \left[ 1 - \exp\left(-\frac{L}{v_1\tau}\right) \right], \quad (8)$$

with  $\tau = 19.7 \text{ ms}$ .<sup>22</sup> Since  $L/(v_1\tau) < 6 \times 10^{-4}$  for  $v_1 > 1100 \text{ m/s}$ , the exponential can be linearized giving

$$N_\tau = \frac{I_0 L}{v_1 \tau}. \quad (9)$$

The spontaneously emitted photon rate is therefore

$$P_0 = 2N_\tau. \quad (10)$$

The channeltron registers

$$P'_0 = \chi N_\tau \quad (11)$$

photons per second. With (9) and

$$I'_0 = b I_0, \quad (12)$$

where  $b$  is the detection efficiency of the multiplier, Eq. (11) gives the relation for the measured rates  $P'_0$  and  $I'_0$

$$P'_0 = \chi \frac{L}{b\tau} \frac{I'_0}{v_1}. \quad (13)$$

Figure 2 shows measured values of  $P'_0$  and  $I'_0$  at several values of  $v_1$ ; the proportionality (13) is obvious.

The photon rates  $P_0$  and  $P'_0$  are practically unchanged for the cell filled with the target gas since elastic forward scattering is dominant. Accordingly, the measured collision-induced photon rate

$$P' = E(v_0) P, \quad (14)$$

with  $E(v_0)$  being the efficiency of the photon detecting system at  $h\nu_0 = 20.6 \text{ eV}$  (where the CRD emission is centered), is obtained as the difference between the photon signals for filled and empty collision cell.

Equation (7) reads for the measured rates

$$\sigma = Q \frac{P'/E(v_0)}{I'_0 |\ln(1-S)| / b}. \quad (15)$$

Combining (15) and (13) yields

$$\sigma = Q \frac{P'}{P'_0} \frac{L\kappa}{|\ln(1-S)| v_1 \tau}, \quad (16)$$

with

$$\kappa = \chi / E(v_0). \quad (17)$$

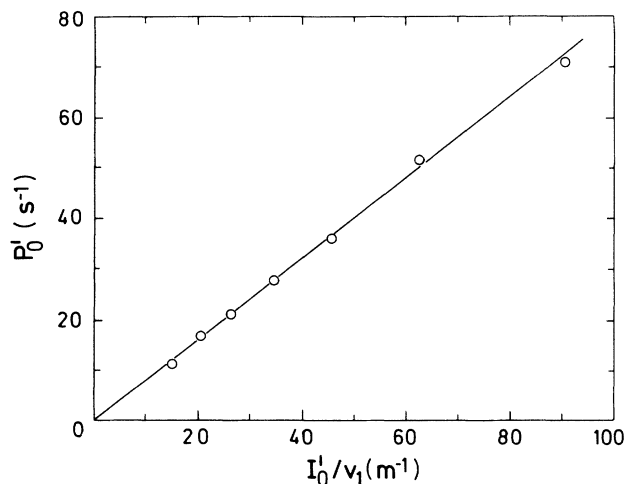


FIG. 2. Plot of the measured natural decay photons  $P'_0$  of  $\text{He}^*(2^1S)$  vs  $I'_0/v_1$  at several  $\text{He}^*(2^1S)$  velocities  $v_1$  with  $I'_0$  being the measured  $\text{He}^*(2^1S)$  intensity.  $\circ$ , measurements; —, eye fit.

$\kappa$  is determined in the Appendix. The result is

$$\kappa = 0.127 \pm 15\% . \quad (18)$$

Formula (16) contains only known and measurable quantities and is used for the determination of the absolute CRD cross sections  $\sigma$  (or  $\sigma_{\text{eff}}$  in the notation of Sec. IV).

#### IV. RESULTS

The circles in Fig. 3 show the measured CRD cross sections for the collision system  $\text{He}^*(2^1S) + \text{He}$  as a function of the  $\text{He}^*$  beam velocity  $v_1$  with the collision cell at  $T = 300$  K. The relative mean collision energies  $\bar{E}$  on the upper scale are calculated according to

$$\bar{E} = \mu(v_1^2 + \frac{3}{2}v_{2w}^2)/2 , \quad (19)$$

where  $\mu$  is the reduced mass and

$$v_{2w} = \sqrt{2kT/m} \quad (20)$$

$$\sigma_{\text{eff}}(v_1) = (\sqrt{\pi}v_{2w}v_1^2)^{-1} \int_0^\infty \sigma(g)g^2 \left[ \exp\left[-\frac{v_1-g}{v_{2w}}\right]^2 - \exp\left[-\frac{v_1+g}{v_{2w}}\right]^2 \right] dg . \quad (21)$$

As Fig. 3 shows, the agreement is fairly good except for the low velocities. In this region, mean cross sections  $\bar{\sigma}$  from rate constants  $r(T)$

$$\bar{\sigma} = r(T)/\sqrt{8kT/\pi\mu} \quad (22)$$

are plotted at the mean energy

$$\bar{E} = 3kT/2 \quad (23)$$

for  $T = 300$  K. The values of  $\bar{\sigma}$  from the three measured

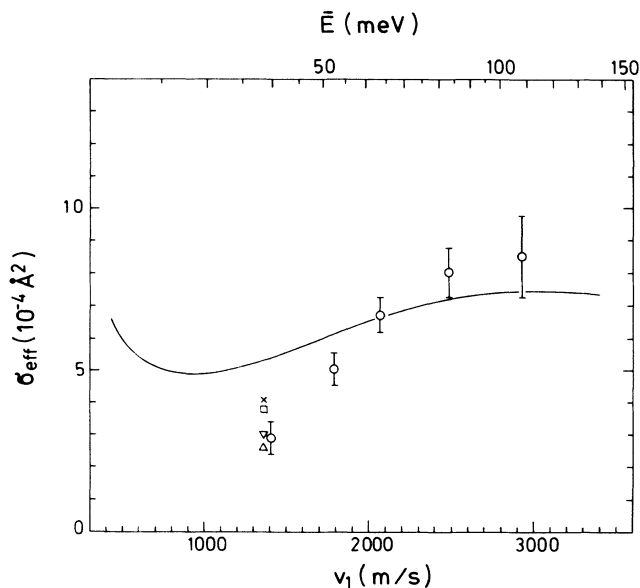


FIG. 3. Energy dependence of the effective CRD cross section  $\sigma_{\text{eff}}$  for  $\text{He}^*(2^1S) + \text{He}$ .  $\circ$ , measurements. Error bars only represent statistical errors; —, quantal calculation of Zygelman and Dalgarno [Ref. 7(d)] averaged for our experimental condition;  $\nabla$ , mean cross section  $\bar{\sigma}$  from Phelps (Ref. 1);  $\triangle$  and  $\square$ ,  $\bar{\sigma}$  from Ref. 2;  $\times$ ,  $\bar{\sigma}$  calculated from  $\sigma(g)$  of Ref. 7(d).

is the most probable velocity of the Maxwellian distribution of the He velocities in the cell ( $k$  is the Boltzmann constant and  $m$  the He mass). The solid curve is based on quantal distorted wave calculations of Zygelman and Dalgarno<sup>7(d)</sup> for the  $A^1\Sigma_u^+$  potential of Jordan and Siska<sup>23</sup> and the  $X^1\Sigma_g^+$  potential of Sando and Dalgarno.<sup>7(b)</sup> These quantal CRD cross sections  $\sigma(g)$  ( $g$  is the relative velocity) account only for the CRD emission near 60 nm. They can therefore be compared with our measurements since both, our Al filter transmission and the CRD emission, sharply decline for longer wavelengths. The comparison is made by averaging the  $\sigma(g)$  curve for our experimental conditions via<sup>24</sup>

rate constants lie close to our CRD cross section. This, however, has to be considered in more detail. The cross in Fig. 3 represents the  $\bar{\sigma}$  value derived via (22) from the value  $r(300\text{ K}) = 7.2 \times 10^{-15} \text{ cm}^3/\text{s}$  which is the result of an  $r$  calculation for the  $\sigma(g)$  values of Zygelman and Dalgarno.<sup>25</sup> Therefore the three measured  $\bar{\sigma}$  values should be shifted upwards. On the other hand, the three measured  $\bar{\sigma}$  values are based on total quenching rates which exceed the quenching emission near 60 nm considered here by about 20%.<sup>7(d)</sup> This implies a downward shift of

the three  $\bar{\sigma}$  values. The net shift is 7% upwards, and the agreement with our measurements is not bad. Nevertheless, it should be mentioned that our low-energy values are difficult to measure since in this regime  $P'_0 \sim 70 \text{ s}^{-1}$  and  $P' \sim 2 \text{ s}^{-1}$ , i.e.,  $P'$  is the result of a difference of nearly equal quantities. Furthermore, there is always a slight systematic drift of the channeltron sensitivity due to a saturation effect from the strong He fluorescence in the open period of the TOF chopper. This drift becomes critical when two nearly equal photon rates for the filled and the empty cell have to be subtracted to get  $P'$ . Finally, there are also remaining uncertainties in the theoretical cross sections which arise from the transition dipole moment adopted for the calculations.<sup>7(d)</sup>

On the whole, however, the agreement between the absolute CRD cross sections from theory and experiment is convincing.

The CRD cross sections for  $\text{He}^*(2^1S) + \text{Ar, Kr, Xe}$  reveal a pronounced decline with decreasing collision energy. Therefore measurements were only performed at a collision energy of 169 meV in the upper energy region. The results for the three collision systems are plotted in Fig. 4 as a function of  $\alpha^2$  where  $\alpha$  is the static dipole polarizability of the corresponding rare-gas target ( $R$ ); the values of  $\alpha$  are taken from Ref. 26. The plot suggests the relation

$$\sigma_{\text{eff}}(\alpha) = c\alpha^2. \quad (24)$$

The same relation was found for the collision systems  $\text{O}^*, \text{S}^*(^1S) + R$ .<sup>8</sup> From Fig. 4, one obtains, for the  $\text{He}^*(2^1S) + R$  systems,  $c = 2.8 \times 10^{-4} \text{ \AA}^{-4}$ .

The CRD cross section of  $\text{He}^*(2^1S) + \text{He}$  is drastically underestimated by (24); this is caused by the special shape of the  $A^1\Sigma_u^+ \text{He}_2^*$  potential: the dominant contribution to the CRD emission comes from distances near the broad  $A^1\Sigma_u^+$  barrier maximum where the excited- and the ground-state potential are parallel, and such details are not contained in (24).

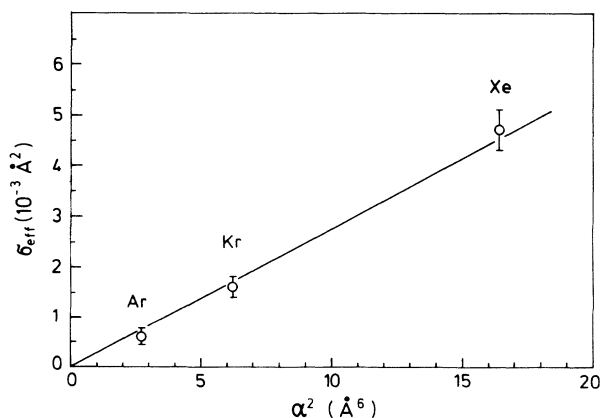


FIG. 4. CRD cross sections at 169-meV collision energy for  $\text{He}^*(2^1S) + \text{Ar, Kr, Xe}$  as a function of  $\alpha^2$  with  $\alpha$  being the static dipole polarizability of the heavier rare gases.  $\circ$ , measurements; —, eye fit (avoiding negative cross sections).

The CRD cross section for  $\text{He}^*(2^1S) + \text{Ne}$  cannot be measured with our method since in this case the CRD emission is totally masked by the huge  $\text{Ne}^*3s_2$  emission<sup>27</sup> which is caused by excitation transfer. Relation (24), however, is applicable to  $\text{He}^*(2^1S) + \text{Ne}$  giving  $\sigma_{\text{eff}} = 4.5 \times 10^{-5} \text{ \AA}^2$  at 169-meV collision energy.

#### ACKNOWLEDGMENTS

We thank Professor A. Dalgarno and Dr. B. Zygelman for their calculations of the quenching cross sections and enlightening discussions. Correspondence with Professor W. R. Hunter, Professor A. V. Phelps, and Professor K. M. Sando is gratefully acknowledged. Discussions with Professor H. Hotop, Professor R. Morgenstern, and Professor H. Morgner were very helpful. Our thanks are due to Professor C. Wulf-Mathies, who supplied us with Sn filters in our first experiments. We express our appreciation to Mr. G. N. Steele and Mr. Forbes Powell from the Luxel Corporation for their excellent Al filters. Numerical calculations were made on the UNIVAC 1108 and the IBM 3090-300E of the Gesellschaft für Wissenschaftliche Datenverarbeitung Göttingen.

#### APPENDIX

The formula for  $\kappa$  is obvious,

$$\kappa = \frac{\chi}{E(\nu_0)} = \frac{\int_0^{\nu_0/2} A(\nu)[E(\nu) + E(\nu_0 - \nu)] d\nu}{\int_0^{\nu_0/2} A(\nu)E(\nu_0) d\nu}. \quad (A1)$$

$A(\nu)$  is the probability for the simultaneous electric-dipole emission of two photons with one photon in the frequency range from  $\nu$  to  $\nu + d\nu$ , and  $E(\nu)$  is the efficiency of the photon-detecting system at the frequency  $\nu$ . The integration limits result from  $A(\nu)$  being symmetric around  $\nu_0/2$ .  $A(\nu)$  is taken from Ref. 21(d). Since<sup>21(d)</sup>

$$\int_0^{\nu_0/2} A(\nu) d\nu = 50.85 \text{ s}^{-1}, \quad (A2)$$

(A1) reduces to

$$\kappa = 1.97 \times 10^{-2} \int_0^{\nu_0/2} A(\nu) \frac{E(\nu) + E(\nu_0 - \nu)}{E(\nu_0)} d\nu. \quad (A3)$$

Figure 5 shows the geometrical configuration of the photon-detecting system. For the sake of clarity the Al filter in front of the channeltron is omitted. Most of the quantities used in the following formulas are evident from this figure. With  $\epsilon(\nu)$  being the channeltron sensitivity and  $T(\nu; l, \phi, \theta)$  the transmission of the filter,  $E(\nu)$  reads

$$E(\nu) = \frac{\epsilon(\nu)}{4\pi L} \int_0^L \int_0^{2\pi} \int_0^{\theta_e(l, \phi)} T(\nu; l, \phi, \theta) \sin\theta \times d\theta d\phi dl. \quad (A4)$$

The integration is only performed for the center line of the metastable beam; this practically gives the average value which one obtains when taking into account the finite lateral dimension of the beam. The upper integra-



- 64, 531 (1976).
- <sup>7</sup>(a) D. C. Allison, J. C. Browne, and A. Dalgarno, *Proc. Phys. Soc.* **89**, 41 (1966); (b) K. M. Sando, *Mol. Phys.* **21**, 439 (1971); **23**, 413 (1972); K. M. Sando and A. Dalgarno, *ibid.* **20**, 103 (1971); (c) A. Z. Devdariani and A. L. Zagrebin, *Opt. Spektrosk.* **61**, 231 (1986) [*Opt. Spectrosc. (USSR)* **61**, 149 (1986)]; (d) B. Zygelman and A. Dalgarno, *Phys. Rev. A* **38**, 1877 (1988).
- <sup>8</sup>P. S. Julienne, M. Krauss, and W. Stevens, *Chem. Phys. Lett.* **38**, 374 (1976); P. S. Julienne, *J. Chem. Phys.* **68**, 32 (1978).
- <sup>9</sup>A. Z. Devdariani and A. L. Zagrebin, *Opt. Spektrosk.* **58**, 1223 (1985) [*Opt. Spectrosc. (USSR)* **58**, 752 (1985)].
- <sup>10</sup>B. Brutschy and H. Haberland, *J. Phys. E* **10**, 90 (1977).
- <sup>11</sup>E. G. Linder and K. G. Hernqvist, *J. Appl. Phys.* **21**, 1088 (1950).
- <sup>12</sup>G. R. Brewer, *J. Appl. Phys.* **30**, 1022 (1959).
- <sup>13</sup>For a detailed description, see G. N. Steele, in *Space Optics*, Proceedings of the 9th International Congress of the International Commission for Optics, Santa Monica, CA, 1972, edited by B. J. Thomson and R. R. Shannon (National Academy of Sciences, Washington, D. C., 1974), p. 367.
- <sup>14</sup>For example, see J. A. R. Samson, *Techniques of Vacuum Ultraviolet Spectroscopy* (Wiley, New York, 1967).
- <sup>15</sup>W. C. Walker, O. P. Rustgi, and G. L. Weissler, *J. Opt. Soc. Am.* **49**, 471 (1959).
- <sup>16</sup>W. R. Hunter, D. W. Angel, and R. Tousey, *Appl. Opt.* **4**, 891 (1965).
- <sup>17</sup>For a detailed description, see J. G. Timothy and L. B. Lapsion, *Appl. Opt.* **13**, 1417 (1974).
- <sup>18</sup>F. Huisken and T. Pertsch, *Rev. Sci. Instrum.* **58**, 1038 (1987).
- <sup>19</sup>R. Feltgen, H. Ferkel, and A. Koch, *Chem. Phys.* **126**, 47 (1988).
- <sup>20</sup>B. Brutschy and H. Haberland, *Phys. Rev. A* **19**, 2232 (1979); F. B. Fiering, S. R. Ryan, and W. H. Wing, *J. Phys. B* **15**, 3841 (1982); S. Burdinski, R. Feltgen, F. Lichterfeld, and H. Pauly, *Chem. Phys. Lett.* **78**, 296 (1981); K. A. Hardy and J. W. Sheldon, *Phys. Rev. A* **30**, 2761 (1984); S. M. Trujillo, in *Proceedings of the Ninth International Conference on the Physics of Electronic and Atomic Collisions, Seattle, 1975*, edited by J. S. Risley and R. Geballe (University of Washington, Seattle, 1975), p. 437; L. Büermann, S. Burdinski, R. Feltgen, and G. Hoffmann, *J. Phys. B* **20**, 2809 (1987); the values for  $\text{He}^*(2^1S) + \text{Kr}$  were obtained by scaling triplet cross sections with  $c_6^{0.4}$  ( $c_6$  is the leading van der Waals constant).
- <sup>21</sup>(a) G. Breit and E. Teller, *Astrophys. J.* **91**, 215 (1940); (b) A. Dalgarno, *Mon. Not. R. Astron. Soc.* **131**, 311 (1966); (c) G. W. F. Drake, G. A. Victor, and A. Dalgarno, *Phys. Rev.* **180**, 25 (1969); (d) V. Jacobs, *Phys. Rev. A* **4**, 939 (1971); (e) F. Bassani and G. Vignale, *Nuovo Cimento* **1D**, 519 (1982).
- <sup>22</sup>R. S. Van Dyck, Jr., C. E. Johnson, and H. A. Shugart, *Phys. Rev. Lett.* **25**, 1403 (1970); *Phys. Rev. A* **4**, 1327 (1971).
- <sup>23</sup>R. M. Jordan and P. E. Siska, *J. Chem. Phys.* **80**, 5027 (1984).
- <sup>24</sup>K. Berkling, R. Helbing, K. Kramer, H. Pauly, Ch. Schlier, and P. Toschek, *Z. Phys.* **166**, 406 (1962).
- <sup>25</sup>It is a well-known fact that  $\sigma_{\text{eff}}$  and  $\bar{\sigma}$  often disagree.
- <sup>26</sup>A. Dalgarno and A. E. Kingston, *Proc. R. Soc. London, Ser. A* **259**, 424 (1960); M. B. Doran, *Z. Phys. B* **7**, 558 (1974).
- <sup>27</sup>C. Dehnbostel, R. Feltgen, and G. Hoffmann (unpublished).
- <sup>28</sup>P. H. Berning, G. Hass, and R. P. Madden, *J. Opt. Soc. Am.* **50**, 586 (1960).
- <sup>29</sup>W. C. Walker, J. A. R. Samson, and O. P. Rustgi, *J. Opt. Soc. Am.* **48**, 71 (1958); O. M. Sorokin, *Opt. Spektrosk.* **16**, 139 (1964) [*Opt. Spectrosc. (USSR)* **16**, 72 (1964)]; O. P. Rustgi, *J. Opt. Soc. Am.* **55**, 630 (1965); O. P. Rustgi, NASA Report No. CR-1096 (National Aeronautics and Space Administration, Washington, D.C., 1968).